CONJUGATE HEAT AND MASS TRANSFER IN A DESICCANT-AIRFLOW SYSTEM: A NUMERICAL SOLUTION METHOD

Yoshihisa Fujii and Noam Lior
Department of Mechanical Engineering and Applied Mechanics, University of Pennsylvania, Philadelphia, Pennsylvania 19104-6315, USA

An effective numerical method was developed for analyzing, as a conjugate problem, transient two-dimensional heat and mass transfer between a solid desiccant and a humid laminar airstream. The method is also more generally applicable to conjugate problems of heat and mass transfer between solids and flowing fluids. The alternating direction implicit (ADI) procedure with an upwind scheme is used for solving both the energy and mass transfer equations. The secant method is applied to solve the local equilibrium relationship between the water content and the water vapor concentration in the silica gel bed. Comparison with conventional, nonconjugate problem solutions has shown that such solutions produce unacceptably large errors in thick-bed (of the order of 2 cm) desiccant systems; for example, they overpredict the water absorption rates by 53%.

INTRODUCTION

It is well known that processes characterized by tightly coupled equations and taking place in interacting spatial domains are best modeled and solved as a conjugate problem. In that way, the interfacial region is not assigned an approximate boundary condition but is included integrally in the solution of the field equations of the interacting domains, and the intereffects among the driving forces in the different domains, as well as property variations, are properly accounted for (cf. [1, 2]). A case in point is the generic problem of heat and mass transfer between a solid and a flowing fluid, such as the problem treated in this paper, involving water vapor transfer between a humid airstream and a desiccant. While the solution here is specific to this problem, the numerical methodology should be suitable for a wide class of problems having similar equations and boundary conditions.

Received 18 September 1995; accepted 8 December 1995.
This study was partially supported by the Pennsylvania Energy Development Authority.
Yoshihisa Fujii's current address is Kajima Corporation, Kajima Technical Research Institute, Chofu-shi, Tokyo 182, Japan.
Address correspondence to Dr. Noam Lior, Department of Mechanical Engineering and Applied Mechanics, University of Pennsylvania, 297 Towne Building, 220 S. 33rd Street, Philadelphia, PA 19104-6315, USA.

1040–7782/96 $12.00 + .00

NOMENCLATURE

b	thickness of silica gel bed, m
c	specific heat, kJ/(kg K)
C	water vapor concentration, (kg water)/(kg mixture)
$\bar{C}$	normalized water vapor concentration $[= (C - C_0)/(C_\infty - C_0)]$
D	water vapor diffusivity in air, m^2/s
E_m	maximum value among the relative errors of water content (w) in the silica gel
E_t	relative error of the computed temperature $[= (T - \hat{T})/(T_\infty - \hat{T})]$
H_1	sorption heat, kJ/kg
k	heat conductivity, kW/(m K)
L	length of silica gel bed, m
$\dot{m}$	water absorption rate into silica gel, kg/(s m^3)
Pr	Prandtl number ($= \nu/\alpha$)
Re	Reynolds number of the airstream ($= u_\infty L/\nu$)
RH	relative humidity
s	constant in Eq. (10)
Sc	Schmidt number ($= \nu/D$)
T	temperature, °C
$\hat{T}$	temperature computed using a 6 × 15 grid and time step of 2 s
u	x component of velocity, m/s
U_∞	free-stream velocity, m/s
v	y component of velocity, m/s
w	water content in the silica gel, (kg water in the silica gel)/(kg silica gel)
α	thermal diffusivity, m^2/s
ε	porosity
ν	kinematic viscosity, m^2/s
ρ	density, kg/m^3

Subscripts

f	fluid, i.e., air
s	silica gel
w	wall, i.e., the silica gel bed
0	initial
∞	outside the boundary layer, free-stream conditions
*	at the interface between the silica gel and the air stream

Desiccants are commonly used to reduce the humidity of airstreams, with a variety of applications including heating, ventilating and air-conditioning, solar-regenerated air-conditioning, and drying of process air [3]. The process obviously involves mass transport of water vapor between the airstream and the desiccant, and it also involves heat transfer because most desiccants, such as the commonly used silica gel, release heat while absorbing water vapor and, at least initially, may differ in temperature from the air/vapor stream to which they are exposed. The convective heat and mass transport in this stream, as well as the temperature and concentration distributions in it and in the desiccant bed, are tightly coupled. Part of the coupling is due to the property dependence on temperature and concentration, most significantly the water absorption characteristics of the silica gel. This indicates that the boundary conditions at the interface between these two media cannot be determined a priori, or imposed, but that the problem should be posed and solved as one of conjugate heat and mass transfer.

The models and numerical analyses of solid-bed desiccant systems reported in the literature (cf. [4–13]) are nonconjugate, typically in that they assume that the desiccant bed is thin enough to ignore internal temperature and concentration distributions, and/or in assigning empirical heat and mass transport rate coefficients at the desiccant-air interface without including the interfacial region in the numerical solution of the field equations.

GOVERNING EQUATIONS

Model Configuration

Figure 1 shows the configuration of the problem treated here. A flat bed packed with silica gel (region I) is placed in a uniform airflow parallel to the bed (region II). One side of the silica gel bed is exposed to the airflow, and the other side is perfectly insulated. The approaching airflow is of uniform velocity U_∞, uniform temperature T_∞, and uniform water vapor concentration C_∞. Initially, the silica gel bed is of uniform temperature T_0, uniform water content w_0, and uniform water vapor concentration C_0.

Basic Equations

Region I: Air and water vapor

Continuity

$$\frac{\partial u}{\partial x} + \frac{\partial v}{\partial y} = 0 \tag{1}$$

Momentum

$$u\frac{\partial u}{\partial x} + v\frac{\partial u}{\partial y} = \nu\frac{\partial^2 u}{\partial y^2} \tag{2}$$

Energy

$$\frac{\partial T}{\partial t} + u\frac{\partial T}{\partial x} + v\frac{\partial T}{\partial y} = \alpha_f\frac{\partial^2 T}{\partial y^2} \tag{3}$$

Mass diffusion (water vapor diffusion in the airflow)

$$\frac{\partial C}{\partial t} + u\frac{\partial C}{\partial x} + v\frac{\partial C}{\partial y} = D_f\frac{\partial^2 C}{\partial y^2} \tag{4}$$

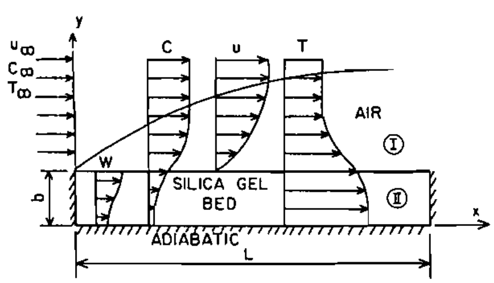

Figure 1. Physical model configuration.

Region II: The silica gel bed

Energy

$$\frac{\partial T}{\partial t} = \alpha_w \left(\frac{\partial^2 T}{\partial x^2} + \frac{\partial^2 T}{\partial y^2} \right) + \frac{H_1 \dot{m}}{c_w \rho_w} \tag{5}$$

where H_1 is the heat of sorption,

$$c_w \rho_w = \varepsilon c_f \rho_f + (1 - \varepsilon) c_s \rho_s \tag{6}$$

and ε is the porosity of the silica gel.

Water vapor diffusion

$$\varepsilon \frac{\partial C}{\partial t} = D_w \left(\frac{\partial^2 C}{\partial x^2} + \frac{\partial^2 C}{\partial y^2} \right) - \frac{\dot{m}}{\rho_f} \tag{7}$$

where $\dot{m}$ is the water absorption rate into the silica gel.

Mass conservation

Water content in the silica gel is expressed as

$$\frac{\partial w}{\partial t} = \frac{\dot{m}}{(1 - \varepsilon) \rho_s} \tag{8}$$

Local equilibrium relation between water content in the silica gel and the water vapor concentration is expressed as

$$C = f(w, T) \tag{9}$$

Equation (9) is an empirical relation, different for each desiccant. For silica gel, according to Ref. [9], the relationship between water content w, temperature T, relative humidity RH, and water vapor concentration C is

$$C = 0.622\text{RH}/(10^s - \text{RH}) \tag{10}$$

where

$$\begin{aligned} \text{RH} = {} & -9.31077 + 0.0017176 51 T_w^2 + 478.0868 w \\ & - 1417.118 w^2 + 2094.818 w^3 + 9.18715 \times 10^{-5} T_1^3 w \end{aligned} \tag{11}$$

and

$$s = 4.21429 - \frac{7.5 T_w}{(237.3 + T_w)} \tag{12}$$

and where T_w is the silica gel temperature (°C) and T_1 is the ambient air temperature (°C).

Summarizing Eqs. (1)–(12), the unknown parameters in the airflow (region I) are u, v, T, and C, and the basic equations are (1)–(4). In the silica gel bed (region II) the unknown parameters are T, C, w, and $\dot{m}$, and the basic equations are (5) and (7)–(9).

The equations were left in their dimensional form because the empirical relation Eq. (9) is a part of the equation system.

Boundary Conditions

Adiabatic bottom surface

$$\frac{\partial T(x,0,t)}{\partial y} = \frac{\partial C(x,0,t)}{\partial y} = 0 \tag{13}$$

Flux continuity

$$k_f \frac{\partial T(x,b,t)}{\partial y} = k_w \frac{\partial T(x,b,t)}{\partial y} \tag{14}$$

$$D_f \frac{\partial C(x,b,t)}{\partial y} = D_w \frac{\partial C(x,b,t)}{\partial y} \tag{15}$$

No slip

$$u(x,0,t) = v(x,0,t) = 0 \tag{16}$$

No heat or mass flux in silica gel bed in the x direction

$$\frac{\partial T(0, y \leqslant b, t)}{\partial x} = \frac{\partial C(0, y \leqslant b, t)}{\partial x} = 0 \tag{17}$$

Upstream conditions

$$T(0,y,t) = T_\infty \tag{18}$$

$$C(0, y > b, t) = C_\infty \tag{19}$$

$$u(0, y > b, t) = U_\infty \tag{20}$$

$$v(0, y > b, t) = 0 \tag{21}$$

No x direction fluxes at $x = L$

$$\frac{\partial T(L,y,t)}{\partial x} = \frac{\partial C(L,y,t)}{\partial x} = 0 \tag{22}$$

Initial Conditions

$$T(x, y, 0) = T_\infty \tag{23}$$

$$C(x, y > b, 0) = C_\infty \tag{24}$$

$$w(x, y \leqslant b, 0) = w_0 \tag{25}$$

$$C(x, y \leqslant b, 0) = C_0 = f(w_0, T_\infty) \tag{26}$$

COMPUTATION METHOD

Velocity Field (in $0 \leqslant x \leqslant L$, $b \leqslant y \leqslant \infty$)

Having assumed constant properties, the flow problem is uncoupled from the problems of heat and mass transfer. The similarity solution is therefore applicable to the laminar flow considered. The Blasius solution is

$$\frac{u_\infty}{U} = F' \tag{27}$$

$$\frac{v}{U_\infty} \frac{\sqrt{U_\infty x}}{v} = \frac{\eta F' - F}{2} \tag{28}$$

where the similarity variable η is defined as

$$\eta = y \frac{\sqrt{U_\infty x}}{v} \tag{29}$$

and the similarity function F is obtained by solving the differential equation

$$F''' + \frac{1}{2} F F'' = 0 \tag{30}$$

with the boundary and initial conditions as defined above for this problem. The values of F and F' are given in the literature.

Numerical Scheme for the Energy Equation

The alternating direction implicit (ADI) method was chosen for the numerical solution of the energy equation primarily because it is unconditionally stable for the two-dimensional parabolic differential equation at hand and because it has second-order accuracy in time and space. Although the method is well described in the literature, some of the details are provided here to elucidate the treatment of the interfacial conditions in this conjugate problem. The interior grid notation is shown in Figure 2.

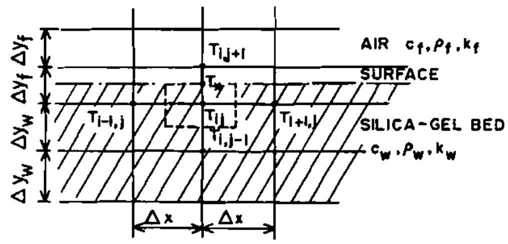

Figure 2. Grid notation and the grid configuration at the solid-gas interface.

In the silica gel bed ($0 \leqslant x \leqslant L$, $0 \leqslant y \leqslant b$). The first half-step is in the x direction:

$$\frac{T_{ij}^{n+1/2} - T_{ij}^{n}}{\Delta t/2} = \alpha_w \left(\frac{T_{i+1,j}^{n+1/2} + T_{i-1,j}^{n+1/2} - 2T_{ij}^{n+1/2}}{\Delta x^2} + \frac{T_{i,j+1}^{n} + T_{i,j-1}^{n} - 2T_{ij}^{n}}{\Delta y_w^2} \right) + \frac{H_1 \dot{m}_{ij}^{n}}{\rho_w c_w} \tag{31}$$

Then

$$-\frac{\alpha_w}{\Delta x^2} T_{i-1,j}^{n+1/2} + \left(\frac{2}{\Delta t} + \frac{2\alpha_w}{\Delta x^2} \right) T_{i,j}^{n+1/2} - \frac{\alpha_w}{\Delta x^2} T_{i+1,j}^{n+1/2} = \frac{\alpha_w}{\Delta y_w^2} T_{i,j-1}^{n} + \left(\frac{2}{\Delta t} - \frac{2\alpha_w}{\Delta y_w^2} \right) T_{i,j}^{n} + \frac{\alpha_w}{\Delta y_w^2} T_{i,j+1}^{n} + \frac{H_1 \dot{m}_{ij}^{n}}{\rho_w c_w} \tag{32}$$

The second half-step is in the y direction:

$$\frac{T_{ij}^{n+1} - T_{ij}^{n+1/2}}{\Delta t/2} = \alpha_w \left(\frac{T_{i+i,j}^{n+1/2} + T_{i-1,j}^{n+1/2} - 2T_{ij}^{n+1/2}}{\Delta x^2} + \frac{T_{i,j+1}^{n+1} + T_{i,j-1}^{n+1} - 2T_{ij}^{n+1}}{\Delta y_w^2} \right) + \frac{H_1 \dot{m}_{ij}^{n}}{\rho_w c_w} \tag{33}$$

Then

$$-\frac{\alpha_w}{\Delta y_w^2}T_{i,j-1}^{n+1} + \left(\frac{2}{\Delta t} + \frac{2\alpha_w}{\Delta y_w^2}\right)T_{ij}^{n+1} - \frac{\alpha_w}{\Delta y_w^2}T_{i,j+1}^{n+1}$$

$$= \frac{\alpha_w}{\Delta x^2}T_{i-1,j}^{n+1/2} + \left(\frac{2}{\Delta t} - \frac{2\alpha_w}{\Delta x^2}\right)T_{ij}^{n+1/2}$$

$$+ \frac{\alpha_w}{\Delta x^2}T_{i+1,j}^{n+1/2} + \frac{H_1 \dot{m}_{ij}^n}{\rho_w c_w} \tag{34}$$

At the solid-gas interface ($0 \leqslant x \leqslant L$, $y = b$). The control volume at the interface of the silica gel and the airstream is shown in Figure 2. The ADI procedure is as follows.

The first half-step is in the x direction:

$$\rho_w c_w \left(\frac{\Delta y_w + \Delta y_f}{2}\right)\Delta x \frac{T_{i,j}^{n+1/2} - T_{ij}^n}{\Delta t/2}$$

$$= k_w\left(\frac{T_{i-1,j}^{n+1/2} + T_{i+1,j}^{n+1/2} - 2T_{ij}^{n+1/2}}{\Delta x}\right)\frac{\Delta y_w + \Delta y_f}{2}$$

$$+ k_w\left(\frac{T_{i,j-1}^n + T_{ij}^n}{\Delta y_w} - \frac{T_{ij}^n - T_*^n}{\Delta y_f/2}\right)\Delta x$$

$$+ H_1 \dot{m}_{ij}\Delta x\left(\frac{\Delta y_w + \Delta y_f}{2}\right) \tag{35}$$

From the heat balance at the surface,

$$\frac{k_w(T_{ij}^n - T_*^n)}{\Delta y_f/2} = \frac{k_f(T_*^n - T_{i,j+1}^n)}{\Delta y_f/2} \tag{36}$$

thus

$$T_*^n = \frac{k_f T_{i,j+1}^n + k_w T_{ij}^n}{k_f + k_w} \tag{37}$$

Substituting Eq. (37) into Eq. (35), we get

$$-\frac{\alpha_w}{\Delta x^2}T_{i-1,j}^{n+1/2} + \left(\frac{2}{\Delta t} + \frac{2\alpha_w}{\Delta x^2}\right)T_{ij}^{n+1/2} - \frac{\alpha_w}{\Delta x^2}T_{i+1,j}^{n+1/2}$$

$$= \frac{2\alpha_w}{\Delta y_w(\Delta y_w + \Delta y_f)}T_{i,j-1}^n + \left(\frac{2}{\Delta t} - \frac{2(\alpha_e \Delta y_f + \alpha_e \Delta y_w)}{\Delta y_w \Delta y_f(\Delta y_w + \Delta y_f)}\right)T_{ij}^n$$

$$+ \frac{2\alpha_w}{\Delta y_f(\Delta y_f + \Delta y_w)}T_{i,j+1}^n + \frac{H_1 \dot{m}_{ij}^n}{\rho_w c_w} \tag{38}$$

where

$$\alpha_w = \frac{k_w}{\rho_w c_w} \tag{39}$$

and

$$\alpha_e = \frac{2k_w k_f}{(\rho_w c_w)/(k_w + k_f)} = \frac{2\alpha_w \alpha_f}{\alpha_w \rho_w c_w/(\rho_f c_f) + \alpha_f} \tag{40}$$

The second half-step is in the y direction. Similar to the procedure in the first half-step,

$$-\frac{2\alpha_w}{\Delta y_w(\Delta y_w + \Delta y_f)} T_{i,j-1}^{n+1} + \left(\frac{2}{\Delta t} + \frac{2(\alpha_w \Delta y_f + \alpha_e \Delta y_w)}{\Delta y_w \Delta y_f(\Delta y_w + \Delta y_f)}\right) T_{ij}^{n+1} - \frac{2\alpha_e}{\Delta y_f(\Delta y_f + \Delta y_w)} T_{i,j+1}^{n+1}$$
$$= \frac{\alpha_w}{\Delta x^2} T_{i-1,j}^{n+1/2} + \left(\frac{2}{\Delta t} - \frac{2\alpha_w}{\Delta x^2}\right) T_{ij}^{n+1/2} + \frac{\alpha_w}{\Delta x^2} T_{i+1,j}^{n+1/2} + \frac{H_1 \dot{m}_{ij}^n}{\rho_w c_w} \tag{41}$$

In the air ($0 \leqslant x \leqslant L$, $y > b$). The upwind scheme is applied for the convective term in the x direction to stabilize the calculation results without having to use a very fine grid system in the x direction.

The first half-step is in the x direction:

$$\frac{2}{\Delta t}\left(T_{ij}^{n+1/2} - T_{ij}^n\right) + u_{ij}\frac{T_{ij}^{n+1/2} - T_{i-1,j}^{n+1/2}}{\Delta x} + v_{ij}\frac{T_{i,j+1}^n - T_{i,j-1}^n}{2\Delta y_f} = \alpha_f \frac{(T_{i,j+1}^n + T_{i,j-1}^n - 2T_{ij}^n)}{\Delta y_f^2} \tag{42}$$

Then

$$-\frac{u_{ij}}{\Delta x} T_{i-1,j}^{n+1/2} + \left(\frac{2}{\Delta t} + \frac{u_{ij}}{\Delta x}\right) T_{ij}^{n+1/2}$$
$$= \left(\frac{\alpha_f}{\Delta y_f^2} + \frac{v_{ij}}{2\Delta y_f}\right) T_{i,j-1}^n + \left(\frac{2}{\Delta t} - \frac{2\alpha_f}{\Delta y_f^2}\right) T_{ij}^n + \left(\frac{\alpha_f}{\Delta y_f^2} - \frac{v_{ij}}{2\Delta y_f}\right) T_{i,j,+1}^n \tag{43}$$

The second half-step is in the y direction:

$$\frac{2}{\Delta t}\left(T_{ij}^{n+1} - T_{ij}^{n+1/2}\right) + u_{ij}\frac{T_{ij}^{n+1/2} - T_{i-1,j}^{n+1/2}}{\Delta x} + v_{ij}\frac{T_{ij+1}^{n+1} - T_{i,j-1}^{n+1}}{2\Delta y_{\mathrm{f}}}$$

$$= \alpha_{\mathrm{f}}\left(\frac{T_{i,j+1}^{n+1} + T_{i,j-1}^{n+1} - 2T_{ij}^{n+1}}{\Delta y_{\mathrm{f}}^2}\right) \tag{44}$$

Then

$$-\left(\frac{\alpha_{\mathrm{f}}}{\Delta y_{\mathrm{f}}^2} + \frac{v_{ij}}{2\Delta y_{\mathrm{f}}}\right)T_{i,j-1}^{n+1} + \left(\frac{2}{\Delta t} + \frac{2\alpha_{\mathrm{f}}}{\Delta y_{\mathrm{f}}^2}\right)T_{ij}^{n+1}$$

$$+\left(-\frac{\alpha_{\mathrm{f}}}{\Delta y_{\mathrm{f}}^2} + \frac{v_{ij}}{2\Delta y_{\mathrm{f}}}\right)T_{i,j+1}^{n+1}$$

$$= \frac{u_{ij}}{\Delta x}T_{i-1,j}^{n+1/2} + \left(\frac{2}{\Delta t} - \frac{u_{ij}}{\Delta x}\right)T_{ij}^{n+1/2} \tag{45}$$

Silica gel bed bottom boundary condition ($0 \leqslant x \leqslant L$, $y = 0$). For the grid $i = 1, 2, \ldots, I$ at $j = 1, 2, \ldots, J$ the adiabatic conditions (no heat flux) are expressed by

$$\begin{aligned} T_{-1,j}^{n} &= T_{2,j}^{n} && i = 1 \\ T_{+I,j}^{n} &= T_{I-1,j}^{n} && \text{at } i = I \\ T_{i,-1}^{n} &= T_{i,2}^{n} && \text{at } j = 1 \\ T_{i,+J}^{n} &= T_{i,J-1}^{n} && j = J \end{aligned} \tag{46}$$

Numerical Scheme for the Mass Transfer Equations

In the silica gel bed ($0 \leqslant x \leqslant L$, $0 \leqslant y \leqslant b$). The first half-step is in the x direction:

$$\frac{2\varepsilon}{\Delta t}\left(C_{ij}^{n+1/2} - C_{ij}^{n}\right)$$

$$= D_{\mathrm{w}}\left(\frac{C_{i+1,j}^{n+1/2} + C_{i-1,j}^{n+1/2} - 2C_{ij}^{n+1/2}}{\Delta x^2} + \frac{C_{i,j+1}^{n} + C_{i,j-1}^{n} - 2C_{ij}^{n}}{\Delta y_{\mathrm{w}}^2}\right) - \frac{\dot{m}_{ij}^{n}}{\rho_{\mathrm{f}}} \tag{47}$$

$$-\frac{D_{\mathrm{w}}}{\Delta x^2}C_{i-1,j}^{n+1/2} + \left(\frac{2\varepsilon}{\Delta t} + \frac{2D_{\mathrm{w}}}{\Delta x^2}\right)C_{i,j}^{n+1/2} - \frac{D_{\mathrm{w}}}{\Delta x^2}C_{i+1,j}^{n+1/2}$$

$$= \frac{D_{\mathrm{w}}}{\Delta y_{\mathrm{w}}^2}C_{i,j-1}^{n} + \left(\frac{2\varepsilon}{\Delta t} + \frac{2D_{\mathrm{w}}}{\Delta y_{\mathrm{w}}^2}\right)C_{ij}^{n} - \frac{D_{\mathrm{w}}}{\Delta y_{\mathrm{w}}^2}C_{i,j+1}^{n} - \frac{\dot{m}_{ij}^{n}}{\rho_{\mathrm{f}}} \tag{48}$$

The second half-step is in the y direction:

$$-\frac{D_w}{\Delta y_w^2}C_{i,j-1}^{n+1} + \left(\frac{2\varepsilon}{\Delta t} + \frac{2D_w}{\Delta y_w^2}\right)C_{ij}^{n+1} - \frac{D_w}{\Delta y_w^2}C_{i,j+1}^{n+1}$$

$$= \frac{D_w}{\Delta x^2}C_{i-1,j}^{n+1/2} + \left(\frac{2\varepsilon}{\Delta t} - \frac{2D_w}{\Delta x^2}\right)C_{ij}^{n+1/2} + \frac{D_w}{\Delta x^2}C_{i+1,j}^{n+1/2} - \frac{\dot{m}_{ij}^n}{\rho_f} \quad (49)$$

At the interface ($0 \leqslant x \leqslant L$, $y = b$). The first half-step is in the x direction:

$$-\frac{D_w}{\Delta x^2}C_{i-1,j}^{n+1/2} + \left(\frac{2\varepsilon}{\Delta t} + \frac{2D_w}{\Delta x^2}\right)C_{ij}^{n+1/2} - \frac{D_w}{\Delta x^2}C_{i+1,j}^{n+1/2}$$

$$= \frac{2D_w}{\Delta y_w(\Delta y_w + \Delta y_f)}C_{i,j-1}^{n+1/2} + \left(\frac{2\varepsilon}{\Delta t} - \frac{2(D_w\Delta y_f + D_e\Delta y_w)}{\Delta y_w\Delta y_f(\Delta y_w + \Delta y_f)}\right)C_{ij}^n$$

$$+ \frac{2D_e}{\Delta y_f(\Delta y_f + \Delta y_w)}C_{i,j+1}^n - \frac{\dot{m}_{ij}^n}{\rho_f} \quad (50)$$

where

$$D_e = \frac{2D_wD_f}{D_w + D_f} \quad (51)$$

The second half-step is in the y direction:

$$-\frac{2D_w}{\Delta y_w(\Delta y_w + \Delta y_f)}C_{i,j-1}^{n+1}$$

$$+ \left(\frac{2\varepsilon}{\Delta t} + \frac{2(D_w\Delta y_f + D_e\Delta y_w)}{\Delta y_w\Delta y_f(\Delta y_w + \Delta y_f)}\right)C_{i,j}^{n+1} - \frac{2D_e}{\Delta y_f(\Delta y_w + \Delta y_f)}C_{i,j+1}^{n+1}$$

$$= \frac{D_w}{\Delta x^2}C_{i-1,j}^{n+1/2} + \left(\frac{2\varepsilon}{\Delta t} - \frac{2D_w}{\Delta x^2}\right)C_{i,j}^{n+1/2} + \frac{D_w}{\Delta x^2}C_{i+1,j}^{n+1/2} - \frac{\dot{m}_{i,j}^n}{\rho_f} \quad (52)$$

In the air ($0 \leqslant x \leqslant L$, $y > b$). The first half-step is in the x direction:

$$-\frac{u_{ij}}{\Delta x^2}C_{i-1,j}^{n+1/2} + \left(\frac{2}{\Delta t} + \frac{u_{ij}}{\Delta x}\right)C_{ij}^{n+1/2}$$

$$= \left(\frac{D_f}{\Delta y_f^2} + \frac{v_{ij}}{2\Delta y_f}\right)C_{i,j-1}^n + \left(\frac{2}{\Delta t} - \frac{2D_f}{\Delta y_f^2}\right)C_{ij}^n + \left(\frac{D_f}{\Delta y_f^2} - \frac{v_{ij}}{2\Delta y_f}\right)C_{i,j+1}^n \quad (53)$$

The second half-step is in the y direction:

$$-\left(\frac{D_f}{\Delta y_f^2} + \frac{v_{ij}}{2\Delta y_f}\right)C_{i,j-1}^{n+1} + \left(\frac{2}{\Delta t} + \frac{2D_f}{\Delta y_f^2}\right)C_{ij}^{n+1}$$

$$+\left(-\frac{D_f}{\Delta y_f^2} + \frac{v_{ij}}{2\Delta y_f}\right)C_{i,j+1}^{n+1} = \frac{u_{ij}}{\Delta x}C_{i-1,j}^{n+1/2} + \left(\frac{2}{\Delta t} - \frac{u_{ij}}{\Delta x}\right)C_{ij}^{n+1/2} \quad (54)$$

Water Content in the Silica Gel [Eq. (8), $0 \leqslant x \leqslant L$, $0 \leqslant y \leqslant b$)]

An explicit scheme is applied for solving Eq. (8):

$$\frac{w_{ij}^{n+1} - w_{ij}^n}{\Delta t} = \frac{1}{(1-\varepsilon)\rho_s}\dot{m}_{ij}^n \quad (55)$$

where w_{ij}^{n+1} must satisfy the local equilibrium

$$C_{ij}^{n+1} = f\left(w_{ij}^{n+1}, T_{ij}^n\right) \quad (56)$$

C_{ij}^{n+1} in Eq. (56) must match the calculation results of Eq. (49). Consequently, Eqs. (48), (49), (55), and (56) must be solved simultaneously. The secant method was employed to determine the water absorption rate $\dot{m}_{ij}^n$. Specifically, the intersection of Eq. (49) and Eq. (55) is obtained iteratively by Eq. (56), where $\dot{m}_1$ and $\dot{m}_2$ are the first guess and C_{11}, C_{12}, C_{21}, and C_{22} are the corresponding concentrations:

$$\dot{m} = \frac{\dot{m}_1(C_{11} - C_{12}) - \dot{m}_2(C_{21} - C_{22})}{\dot{m}_2 - \dot{m}_1} \quad (57)$$

Figure 3 shows the program logic flow diagram.

COMPUTATION EXAMPLE

Physical Data and Grid System

Table 1 lists the physical data for the air and the silica gel bed, used in the computational example.

Computations of the effect of grid size on solution accuracy were performed, and the results are shown in Figures 4*a* and 4*b*. $\hat{T}$ is the computation result using the finest grid system, 25 × 15. As expected, a finer grid system is required in the y than in the x direction. The 15 × 6 grid was chosen as a good compromise of computational time and accuracy. The relative error in temperature is then $< 5\%$.

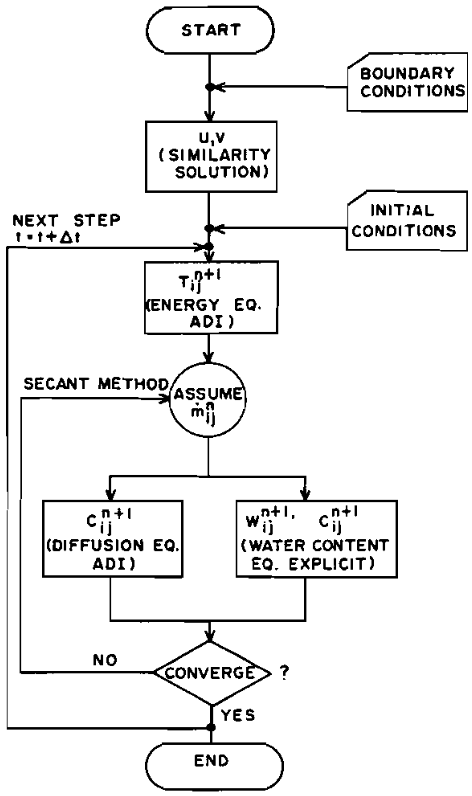

Figure 3. Program logic flow diagram.

Time Step

Figure 4*c* shows the relationship between the relative temperature error E_T and the computation time step Δt. The relative error was found to be $< 1\%$ for $\Delta t > 5$ s. It is worth noting that since the number of iterations of the secant method increases with the magnitude of the time step, larger time steps do not always reduce the overall computation time. The time step chosen for these computations was 2 s.

The program was developed to be efficient: computation for an hour of physical process time is performed in an order of minutes on a personal computer.

Convergence of the Secant Method

Figure 5 shows the convergence performance of the secant method used to solve the equations for the water content of the silica gel bed, Eqs. (47), (48), and (54)–(56). In the figure the maximum error (E_m) is defined as the maximal value

Table 1. Physical data for the computation example

Parameter	Nomenclature	Value
Length of silica gel bed	L	0.05 m
Thickness of silica gel bed	b	0.02 m
Porosity of silica gel bed	ε	0.1
Density of air	ρ_f	1.2 kg/m^3
Density of silica gel	ρ_s	1060 kg/m^3
Specific heat of air	c_f	1.01 kJ/(kg k)
Specific heat of silica gel	c_s	0.904 kJ/(kg k)
Kinematic viscosity of air	ν_f	1.50×10^{-5} m^2/s
Thermal diffusivity of air	α_f	2.21×10^{-5} m^2/s
Thermal diffusivity of silica gel bed	α_w	8.80×10^{-5} m^2/s
Water vapor diffusivity in air	D_f	2.79×10^{-5} m^2/s
Water vapor diffusivity in silica gel bed	D_w	2.79×10^{-5} m^2/s
Sorption heat	H_l	2.550 kJ/kg
Airstream velocity	U_∞	0.1, 0.5 m/s
Airstream temperature	T_∞	30°C, 80°C
Airstream water vapor concentration	C_∞	0.0276 (RH 100% at 30°C)
Initial water content	w_0	0.1
Prandtl number of airstream	Pr	0.72 (@30°C)
Schmidt number	Sc	0.56 (vapor in air)
Reynolds number of airstream	Re	$< 1.58 \times 10^3$

among the relative errors at all grid points in the silica gel bed. Approximately 50 iterations are required for an accuracy (E_m) of the order of 10^{-2}. Fifty iterations were used in the program.

COMPARISON BETWEEN CONJUGATE AND NONCONJUGATE SOLUTIONS

It is obviously easier to solve the nonconjugate problem because it is then not necessary to simultaneously solve the heat conduction and mass diffusion equations in the silica gel bed, and the momentum and convective heat and mass transfer equations in the airstream. Furthermore, the boundary conditions at the silica gel/air interface are then simply specified a priori without the need for formulating and solving conservation equations at that interface. As stated in the introduction, most of the past solutions of desiccant problems have indeed been nonconjugate, ignoring the heat and mass transfer in the silica gel bed and just using the absorptive properties of the silica gel as a boundary condition. It is thus of great interest to compare the solutions of the conjugate and nonconjugate problems and to determine the extent of improvement in information obtained by going through the extra effort of solving the conjugate problem.

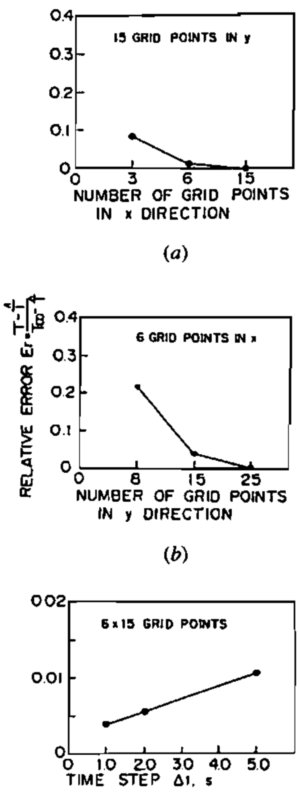

Figure 4. Relative error (E_r) in the computed temperature as a function of grid size and time step. $\hat{T}$ is the temperature computed using the finest grid system, 25×15.

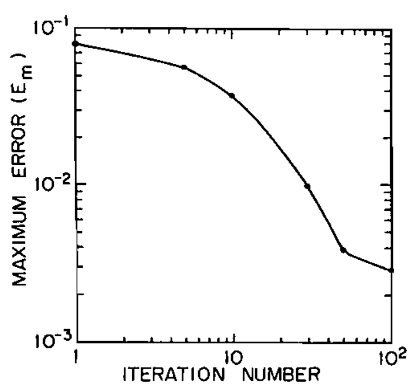

Figure 5. Convergence of the secant method used to solve the silica gel water content equations. E_m is the maximum among the relative errors in the computational domain.

The nonconjugate problem in this case is made equivalent to the conjugate problem, with the condition that $\alpha_w \to \infty$ and $D_w \to \infty$, where α_w is the thermal diffusivity in the silica gel bed and D_w is the water vapor diffusivity in the silica gel bed. The nonconjugate problem was solved here for $u_\infty = 0.1$ m/s, $T_\infty = 30$°C, and $C_\infty = 0.0276$, with α_w and D_w taken to be 3 orders of magnitude larger than their actual physical values listed in Table 1.

Considerable differences were found between all of the results of the nonconjugate and conjugate problems, in part because of the strong relationship between the local temperature and water absorption rate. For example, Figure 6 shows the transient temperatures and the transient volume-averaged absorption rates defined as

$$\overline{m} = \frac{1}{bL}\int_0^b \int_0^L \dot{m}(x,y)\,dy\,dx \tag{58}$$

At the beginning of the process the silica gel temperature increases sharply owing to absorption heat. Eventually, it reaches a maximum at which the surface temperature is high enough for heat removal by the airflow to balance the heat

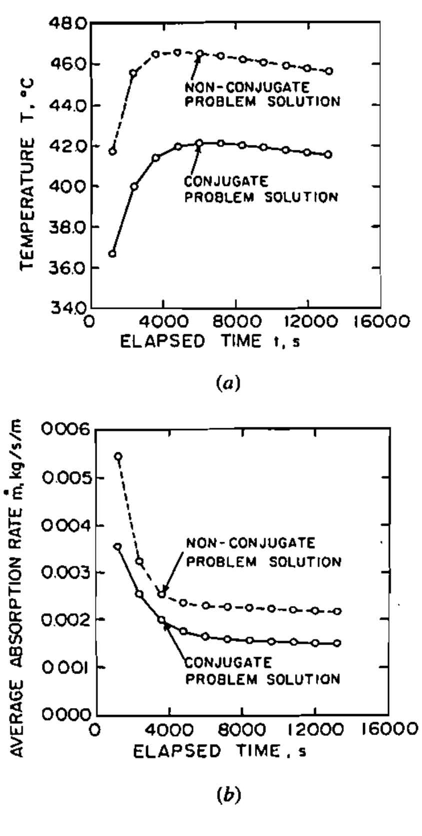

Figure 6. Comparison of results from conjugate and nonconjugate solutions at $x = 0.03$ m. Free-stream conditions are u_∞ 0.1 m/s, $T_\infty = 30$ °C, and $C_\infty = 0.0276$: (*a*) interface temperature and (*b*) average water absorption rate.

generation. At the same time, as the silica gel absorbs water, the vertical concentration gradient keeps decreasing and, consequently, the absorption rate also decreases. This causes the surface temperature to start declining after it has reached its maximum.

In the range of parameters considered, the temperatures from the solution of the nonconjugate problem are seen to be approximately 5°C higher than those of the conjugate problem. In other words, the temperature excess, $T_s - T_w$, determined from the nonconjugate problem is about 87% larger than that determined from the conjugate problem. Solution of the nonconjugate problem also overpredicts the average absorption rate by up to 53%. One can thus see that the conventional, nonconjugate heat and mass transfer solution of thick-bed (of the order of 2 cm) desiccant dehumidification is likely to introduce large errors and that the problem should thus be treated as conjugate.

CONCLUSIONS

An effective method was developed for solving the transient two-dimensional conjugate flow and heat and mass transfer problems in solid desiccants subjected to laminar humid airflow. The technique applies the ADI method with an upwind scheme for the convective terms to both the energy and the mass diffusion equations. The secant method is applied to solve the local equilibrium relationship between the water content and the water vapor concentration at each grid point in the silica gel bed. Hours of real-time results require only a few minutes of computation on a PC.

The extra effort in computing the conjugate problem is well worth it for thick-bed (here, of the order of 2 cm) desiccants. In comparison, nonconjugate problem solutions were found to produce large errors; for example, they overpredict the water absorption rates by 53%.

REFERENCES

1. G. F. Jones and N. Lior, Conjugate Heat Transfer and Flow Distribution in an Assembly of Manifolded Finned Tubes, in J. B. Kitto Jr. and J. M. Robertson (eds.), *Maldistribution of Flow and Its Effect on Heat Exchanger Performance*, ASME HTD-vol. 75, pp. 127–136, ASME, New York, 1987.
2. N. Lior and Y. Fujii, On Conjugate Heat Transfer in Crystal Growth, in I. Tanasawa and N. Lior (eds.), *Heat and Mass Transfer in Materials Processing*, pp. 217–243, Hemisphere, New York, 1992.
3. A. A. Pesaran, T. R. Penney, and A. W. Czanderna, Desiccant Cooling: State of the Art Assessment, National Renewable Energy Laboratory Rept. NREL/TP-254-4147, Golden, Colo., 1992.
4. P. J. Banks, Coupled Equilibrium Heat and Single Adsorbate Transfer in Flow Through a Porous Medium, I: Characteristic Potentials and Specific Capacity Ratios, *Chem. Eng. Sci.*, vol. 27, pp. 1143–1155, 1972.
5. D. J. Close and P. J. Banks, Coupled Equilibrium Heat and Single Adsorbate Transfer in Fluid Flow Through a Porous Medium, II: Predictions for a Silica-Gel Air-Drier Using Characteristic Charts, *Chem. Eng. Sci.*, vol. 27, pp. 1157–1168, 1972.

6. I. L. Maclaine-Cross and P. J. Banks, Coupled Heat and Mass Transfer in Regenerators—Prediction Using an Analogy with Heat Transfer, *Int. J. Heat Mass Transfer*, vol. 15, pp. 1225–1241, 1972.
7. D. Roy and D. Gidaspow, Nonlinear Coupled Heat and Mass Exchange in a Cross-Flow Regenerator, *Chem. Eng. Sci.*, vol. 29, pp. 2101–2114, 1974.
8. R. B. Holmberg, Combined Heat and Mass Transfer in Regenerators with Hygroscopic Materials, *J. Heat Transfer*, vol. 101, pp. 205–210, 1979.
9. V. C. Mei and Z. Lavan, Performance of Cross-Cooled Desiccant Dehumidifiers, *ASME J. Solar Energy Eng.*, vol. 105, pp. 300–304, 1983.
10. A. A. Pesaran and A. F. Mills, Moisture Transport in Silica Gel Packed Beds, I: Theoretical Study, *Int. J. Heat Mass Transfer*, vol. 30, pp. 1037–1049, 1987.
11. P. Gandhidasan, M. R. Ullah, and C. F. Kettleborough, Analysis of Heat and Mass Transfer Between a Desiccant-Air System in a Packed Tower, *ASME J. Solar Energy Eng.*, vol. 109, pp. 89–93, 1987.
12. W. Zheng and W. M. Worek, Numerical Simulation of Combined Heat and Mass Transfer Processes in a Rotary Dehumidifier, *Numer. Heat Transfer Part A*, vol. 23, pp. 211–232, 1993.
13. K. D. Kafui, Transient Heat and Moisture Transfer in Thin Silica Gel Beds, *J. Heat Transfer*, vol. 116, pp. 946–953, 1994.